Saudi Pharmaceutical Journal 30 (2022) 585–594

Contents lists available at ScienceDirect

Saudi Pharmaceutical Journal

journal homepage: www.sciencedirect.com

iTRAQ-derived quantitative proteomics uncovers the neuroprotective property of bexarotene in a mice model of cerebral ischemia–reperfusion injury

Hailin Liu [a], Hu Wang [a], Sisi Chen [b], Shengwei Liu [c], Xiaocui Tian [c], Zhi Dong [c], Lu Xu [d,*]

[a] Department of Pharmacy, First people's Hospital of Chongqing Liangjiang New Area, Chongqing 401121, China
[b] School of Clinical Medicine, Chongqing Medical and Pharmaceutical College, Chongqing, China
[c] Department of Pharmacology, Chongqing Medical University, the Key Laboratory of Biochemistry and Molecular Pharmacology, Chongqing 400016, China
[d] School of Pharmacy, Chongqing Medical and Pharmaceutical College, Chongqing 41331, China

ARTICLE INFO

Article history:
Received 26 October 2021
Accepted 21 February 2022
Available online 25 February 2022

Keywords:
Bexarotene
Cerebral ischemia reperfusion injury
iTRAQ
Apoptosis
JIP3

ABSTRACT

Bexarotene, a FDA-approved drug for cutaneous lymphoma, has been shown to exert brain protective effects. In previous study, we demonstrated that Bexarotene protects against cerebral ischemic stroke by suppressing the JNK/Caspase-3 signaling pathway. However, the molecular mechanisms by which Bexarotene-mediated neuroprotective are not fully understood. Based on the isobaric tags for relative and absolute quantification (iTRAQ)-derived proteomics and bioinformatics analysis, 4,454 differentially expressed proteins (DEPs) were identified in upstream of the JNK signaling pathway. Among them, 149 DEPs showed aberrant expression in the vehicle-versus Bexarotene-treated mice. DEPs were primarily enriched in the metabolism, calcium, and MAPK signaling pathways. The largest DEP increase was seen with heat shock protein HSP 70, whereas the largest DEP decrease was seen with JNK scaffold protein JIP3, both of which are involved in the MAPK network. Furthermore, we illustrated the Bexarotene obviously abolished oxygen and glucose deprivation/reperfusion (OGD/R)- induced LDH leakage, cells apoptosis, and the protein expression level of the JIP3,p-ASK1, p-JNK, and Cleaved Caspase3. Together, these results suggest a potential neuroprotective role of Bexarotene via inhibition of the JIP3/ASK1/JNK/Caspase 3 signaling pathway.

1. Introduction

Stroke, one of a major diseases threatening human health. It has the characteristics of high incidence, disability, and mortality (Campbell et al., 2019). The 2018 Global Burden of Stroke reported that stroke has become the second most serious disease-causing death world-wide, and ischemic stroke is more frequent, about accounts for>80% of this form of disease (Katanet al., 2018).

Emerging reports, from both basic and clinical investigations, suggest that Cerebral Ischemic-Reperfusion (CIR) injury involves a variety of pathophysiological processes, including release of excitatory amino acids, intracellular Ca^{2+} overload, oxygen free radical damage, autophagy, and cell apoptosis (Baek et al., 2014). These pathophysiological processes are closely related to therapeutic efficacy and patient prognosis. Unfortunately, despite numerous basic and clinical investigations on this topic, at home and abroad, there still exists a lack of an effective neuroprotective drug that can improve the outcome of ischemic stroke. Therefore, continuous exploration into the development of highly efficacious drugs for the treatment of ischemic stroke has important research and clinical implications.

Bexarotene is a new type of retinoic acid analogue, which exerts an anti-tumor effect via selective interaction with the three subunits of retinoid X receptor (RXR): RXRα, RXRβ, and RXRγ. Bexarotene possesses the properties of small molecular weight (348.48KD), high fat solubility, and easy penetration through the blood–brain barrier (BBB) (Xu et al., 2015). Recently, multiple evidence have highlighted the protective effect of Bexarotene against central nervous system diseases. Zhou et al. (Zhou et al., 2015), for

* Corresponding author at: Department of Pharmacology, Chongqing Medical and Pharmaceutical College, Chongqing 401331, China.
E-mail address: 106334600@qq.com (L. Xu).

Peer review under responsibility of King Saud University.

Production and hosting by Elsevier

https://doi.org/10.1016/j.jsps.2022.02.012
1319-0164/

instance, reported that Bexarotene reduced neuroinflammation and improved neurological deficits after the subarachnoid hemorrhage (SAH) by regulating the PPARγ/SIRT6/Fox-O3a signaling pathway in the SAH model of Sprague Dawleyrats. Similarly, Zhong et al. (Zhong et al., 2017) revealed that Bexarotene increases the expression of long non-coding RNAs (lnc RNAs) via RXR-α subtype and exerts anti-inflammatory and anti-apoptotic pharmacological effects. Moreover, Xu et al. (Xu et al., 2015) demonstrated, in the CIR rat injury model, that Bexarotene significantly reduces brain injury via reduction ofbrain matrix metalloproteinase(MMP)-9 activity and elevation of the BBB tight junction proteins Claudin-5 and Occludin levels. Huuskonen et al. (Huuskonen et al., 2016) proposed that Bexarotene reduces tissue damage and behavioral scores of thrombotic stroke in elderly mice by regulating autophagy. Furthermore, our previous study revealed that Bexarotene inhibits activation of the JNK/Caspase 3 axis, reduces neuronal apoptosis at the brain injury site, and reduces CIR injury (Liu et al., 2019).

The protective mechanism of Bexarotene on brain injury is multifaceted. Most published reports explored only one side of the protective effect of Bexarotene on CIR. Therefore, a macroscale investigation exploring multiple targets and pathways is highly warranted. Here, in the transient middle cerebral artery occlusion (t-MCAO) model, we adopted the quantitative proteomics method of (isobaric tags for relative and absolute quantification) iTRAQ, combined with LC-MS/MS, to conduct a comprehensive study on the Bexarotene-mediated protection against CIR damage.

2. Materials and methods

2.1. Materials

Bexarotene was purchased from Abcam Bio-tech (Cambridge, MA, UK). The immortalized mouse hippocampal neuron line (HT22) was obtained from JENNIO Biological Technology (Guangzhou, China).The sodium dodecyl sulfate (SDS), Acr-Bis, Bovine serum albumin (BSA) were purchased from GEN-VIEW SCIENTIFIC Inc (Florida, USA). The Tunelkit , Phosphate Buffer Saline (PBS) , Tris-HCl buffer, Methyl Thiazolyl Tetrazolium (MTT), Fetal bovine serum (FBS), Dulbecco's Modified Eagle Medium/Nutrient Mixture F-12(DMEMF-12) and Dulbecco's modified Eagle's medium (DMEM) were purchased from Dingguo Co. Ltd. (Beijing, China). Antibodies against JIP1, JIP3, phospho-JNK (1/2), phospho-ASK1, ASK1, Cleaved Caspase 3 were purchased from Cell Signaling Technology (Danvers, MA, USA). Antibodies against β-actin and horse radish peroxide (HRP)-conjugated goat anti-rabbit IgG (H + L) were purchased from Proteintech Biotechnology (Proteintech, Wuhan, China). The plasimid vector of pCDNA 3.1 was purchased from Gene Create Biological Engineering (Wuhan, China).

2.2. Animal models and drug treatment

2.2.1. Animals

Ninety male C57BL/6 male mice, aged 8–12 weeks, weighing 20–25 g, were obtained from the Animal Laboratory Center of Chongqing Medical University (Chongqing, China). Mice were housed each group in one cage with a temperature-controlled (25 ± 1 °C) and maintained on standard food and water available adlibitum. The animal experiment was in accordance with the guidelines of the National Institutes of Health and were approved by the Experimental Ethics Committee of Chongqing Medical University (License number: SYXK YU 2010–001).

2.2.2. Transient focal cerebral ischemia model

Focal cerebral ischemia was produced by t-MCAO, as previously described (Liu et al., 2019). Briefly, animals were anesthesiaed with 3% isoflurane in a 67%/30% mixture of N_2O/O_2, and 1.5% of isoflurane was present during the surgery to maintain the anesthesia, and were placed in a supine position subsequently. Underan operating microscope, the right common carotid artery (CCA), the external carotid artery (ECA), and the internal carotidartery (ICA) were exposed. Subsequently, the CCA and ECA were ligated. A silicone-coated nylon filament was inserted into the internal carotid artery through the incision and advanced 10–12 mm distal to the carotid bifurcation, to reach the point of origin of the middle cerebral artery. The nylon filament was taken out after 60 min of occlusion to allow reperfusion. The rectal temperature was maintained at 37.0 ± 0.5 °C throughout the surgery with a temperature-controlled heating pad.

2.2.3. Bexarotene treatment and experiment groups

The solution of Bexarotene (#ab141025, Abcam, Cambridge, UK) was prepared as previously described (Zhong et al., 2017), Briefly, Bexarotene was dissolved in dimethylsulfoxide (DMSO), and the mixed solution was prepared with polyethylene glycol (15)-hydroxystearate (Solutol), ethanol, and water with a ratio of 15:10:75subsequently. The final concentration of Bexarotene was 0.50 mg/mL.

Mice were randomly divided into the following groups: the Sham-operated (S), vehicle-treated (V), Bexarotene-treated (B). Both V and B mice underwent t-MCAO for the establishment of CIR injury, whereas S mice underwent the same operation, but without the insertion of the thread plug. B mice received Bexarotene (5 mg/kg) immediately after surgery and every day after that, at a pre-set time point, via intraperitoneal injection. V mice were administered equal amount of vehicle solvent, whereas the sham S mice did not receive any Bexarotene or vehicle solvent intervention.

2.3. Cell culture

Hippocampal neuronal cell line (HT22) cells were maintained inDMEMF-12 with 10% FBS at 37℃ and 5% CO_2, 75 %N_2, and 20% O_2 in a humidified incubator. Prior to experimentation, the cells were exposed to oxygen-glucose deprivation/reperfusion (OGD/R). Briefly, the cells were phosphate-buffered saline (PBS)-rinsed, and maintained glucose-free and serum-free medium, and kept in incubator conditions as follows: 37 ℃, 5% CO_2, 1% O_2, and 94 % N_2 for 2 h. Subsequently, the medium was replaced with normal medium, with or without bexarotene, and the cells were placed back in the normoxic incubator for reoxygenation. Control cells were treated the same way, but without OGD/R.

2.4. Plasmid transfection

JNK-interacting protein 3 (JIP3)-overexpressing plasmid were constructed. Prior to transfection, the cells were maintained in DMEM with 10% fetal bovine serum (FBS) until the cell density was up to 70–80%. Next, 2 μl lipo 2000 transfection reagent and 0.4 μg of JIP3 plasmid was respectively diluted in 50 μl serum-free DMEM medium. Then, both mixtures were combined and left at room temperature for 20 min, prior to the addition of 100 μl of serum-free DMEM. The total of 200 μl complex transfection medium was then introduced to the cells for 5-hour at 37℃. Following this, the medium was replaced with 0.5 ml DMEM carrying10% FBS, then incubated for 48-hour. The control group cells underwent the same process, without the addition of the JIP3-overexpressing plasmid.

2.5. Proteomics

2.5.1. Protein sample preparation

Brain tissue of the infarct side were first dissolved in 200 μl Triethylammonium bicarbonate (TEAB) dissolution buffer, and sonificated for 15 min, then centrifuged at 12000 × *g* for 20 min. The supernatant was retrieved and introduced to 4-fold volume chilled acetone with 10 mM Dithiothreitol (DTT) for 2 h, then centrifuged again at 12000 × *g* for 20 min at 4 °C. The resulting pellet was then combined with 800 μl chilled acetone at 56 °C to dissolve the protein disulfide bonds, and centrifuged again at 12000 × *g* for 20 min at 4 °C before drying. The dried pellet was then re-suspended in 100 μl TEAB dissolution buffer and kept at −80 °C until further examination.

2.5.2. Digestion and desalting

The total protein concentration was measured using the Bradford method. For each sample, 100 μg of protein was dissolved to 100 μl dissolution buffer and diluted 5 times with 100 mM TEAB, and then trypsin (V5280, Promega) was added according to the mass ratio of 1:50 (trypsin: protein). Enzymolysis was carried out overnight at 37℃. The hydrolyzed peptide was desalted by C18 column, and the desalted peptide was vacuum freeze-dried.

2.5.3. iTRAQ labeling

Sample labeling was done with iTRAQ Reagent-8 plex Multiplex Kit (AB Sciex U.K. Limited). The samples and labeled markers are presented in Table1. All labeled samples were prepared with the same amount and fractionated with high-performance liquid chromatography (HPLC) system (Thermo DINOEX Ultimate 3000 BioRS), using a Durashell C18(5 μm, 100 Å, 4.6x250 mm). The peptide was separated by gradually increasing ACN concentration under alkaline conditions, with the flow rate 1 ml/min. And one tube was collected every minute. A total of 42 secondary fractions were collected and combined into 12 components (each component 3.5 ml). The combined component was desalted on Strata-X column and dried in vacuum.

2.5.4. LC-MS/MS analysis

LC-ESI-MS/MS evaluation was done with an AB SCIEX nano LC-MS/MS (Triple TOF 5600 plus) system. Samples underwent chromatography with a gradient from 2 to 30% (buffer A 0.1% (v/v) formic acid, 5% (v/v) acetonitrile, buffer B 0.1% (v/v) formic acid, 95% (v/v) acetonitrile), following direct injection onto a 20 μm PicoFrit emitter (New Objective) packed to 12 cm with Magic C18 AQ 3 μm 120 Å stationary phase. Then, MS1 spectra were recorded at 350–1,500 *m*/*z* for 250 ms and the 20most intense precursors, with charge state 2–5, were chosen for fragmentation. MS2 spectra were recorded at 50–2,000 *m*/*z* for 100 ms; with precursor ions exclusion from reselection for 15 s.

2.5.5. Proteomics data analysis

Raw LC-MS/MS data was analyzed using ProteinPilot Software v4.5, with the following parameters: Triple TOF 5600 instrument, iTRAQ quantification, cysteine modification with iodoacetamide, biological modifications chosen as ID focus, trypsin digestion, Quantitate, and protein quantification and normalization after bias and background. To calculate false discovery rate (FDR), an automated decoy database screening and the PSPEP (Proteomics System Performance Evaluation Pipeline Software, integrated in the Protein Pilot Software) algorithm were employed. The following conditions met the strict DEPs criteria: unique peptides ≥ 2, with average ratio-fold change > 1.5 (up-regulation), and < 0.67 (down-regulation), as well as p-value < 0.05.

2.6. Bioinformatics analysis

The network for GeneOntology (GO) mapping and annotation was generated and analyzed using Clu GO from Cytoscape 3.7.2. DEPs pathway enrichment analysis was conducted with the Kyoto Encyclopedia of Genes and Genomes (KEGG) database and Database for Annotation. P-value < 0.05 was defined as statistically significant.

2.7. MTT assay

This was used for the evaluation of cell viability after Bexarotene treatment, under both normal and OGD conditions. Bexarotene (#ab141025, Cambridge, UK) was dissolved in DMSO, and subsequently diluted with culture medium to different concentrations. HT22 cells were arbitrarily assigned to 4 groups: Control; Control + Bexarotene; OGD/R and OGD/R + Bexarotene. OGD/R, where the cells were placed under OGD for 2 h, followed by incubation in normal medium and in normoxic incubator for 12 h. Briefly, 6,000 HT22 cells/well were incubated in 96-well plates overnight, and treated with differing concentrations of Bexarotene (0.1, 0.3, 1, 3, 9, 27 , and 81 μM), in the presence or absence of OGD. Subsequently, the treated cells were exposed to 5 mg/mL MTT reagent for 4 h at 37℃ and the formed crystals were dissolved in 150 μl of dimethylsulfoxide (DMSO), Absorbance was measured at 490 nm, using a PR 4100 microplate reader.

2.8. Cell cycle and apoptosis analysis usingflow cytometry

1×10^6 per ml HT22 cells were added to 6-well plates, as previouly reported (Yan et al,. 2017). Subsequently, the cells were digested with 0.125% trypsin, rinsed three times in cold PBS, and resuspended in phosphate buffer solution, Then, cells were stained with fluoresce in isothiocyanate-conjugated annexin V for 10 min at room temperature, then followed by centrifugation and resuspened in binding buffer mixed with PI (1 mg/ml). Lastly, cellular apoptotic rate was assessed via flow cytometry (Cytoflex S, BD Bioscience company).

2.9. Quantitative real-time PCR

The total RNA of HT22 cells was collected by RNAiso Plus and reverse-transcribed into cDNA using the iScript cDNA synthesis kit according to the manufacturer's protocols. Gene-specific oligonucleotide primers for qRT-PCR were used as follows: β-actin, 5′-CCACCATGTACCCAGGCATT-3′ (forward) and 5′-CGGACTCATCG

Table 1
Screening results of DEPs.

Group	Total Proteins	Up-regulated DEPs	Down-regulated DEPs	Totle DEPs
B/V	4381	138	11	149
B/S	4380	59	6	65
V/S	4376	86	136	222

(S: Sham-operated , V: vehicle-treated , B: Bexarotene-treated .).

TACTCCTGC-3′(reverse); JIP1,5′-ACTGTCCTACGACTCGGTCA-3′ (forward) and 5′-CATACTCCTCACCAATGGCT-3′ (reverse); and JIP3, 5′-GCAGATCAGATTTCCCGACT-3′ (forward) and 5′-CTGCTTTCTGT TTGGCCGCTA-3′ (reverse).The relative expression level was of JIP1 and JIP3quantified using the $2^{(-\triangle\triangle Ct)}$ method.

2.10. Western blot analysis

Cell homogenate was centrifuged at 12,000 × *g* for 5 min at 4 °C and the supernatant was obtained. Protein quantification was done with a bicinchoninic acid protein assay kit (P0012S, Beyotime, China) and 50ug protein was separated by 8% sodium dodecyl sulfate polyacrylamide gel electrophoresis (SDS-PAGE), and transfer to a polyvinylidene fluoride (PVDF) membrane (Millipore, USA).The membranes were blocked in 5% BSA for 1 h at room temperature, and incubated overnight at 4 °C with the following primary antibodies: rabbit monoclonal anti-JIP1 (#14568–1-AP, Proteintech, 1:1000), rabbit monoclonal anti-JIP3 (#25212–1-AP, Proteintech, 1:1000), rabbit monoclonal anti-phospho-JNK(1/2) (#4668, Cell Signaling Technology, 1:1000), rabbit monoclonal anti-phospho-ASK1 (#28846–1-AP, Proteintech, 1:1000), rabbit monoclonal anti-ASK1 (#28201–1-AP, Proteintech, 1:1000), rabbit polyclonal anti-Cleaved Caspase-3 (#ab49822, Abcam, 1:1000), and β-actin (#66009–1-Ig, Proteintech, 1:3000). Membranes were then washed by three TBST and incubated with, HRP-conjugated secondary antibodies (#SA00001-2, Proteintech, 1:5000) at room temperature for 1 h. Three more TBST rinses, and, finally, protein detection with the enhanced chemiluminescence detection system (Bio-Rad, Hercules, CA, USA).

2.11. Statistical analysis

All results were expressed as the means ± standard deviation (SD), Statistical analyses were performed with the SPSS 17.0 software (IBM Corp, Chicago, IL, USA). Comparisons among different groups were performed with one-way analysis of variance (ANOVA) followed by Tukey's test. P values < 0.05 was represented as statistically significant.

3. Results

3.1. DEPs screening

4,454 proteins in brains of mice in Sham, Vehicle and Bexarotene treated groups were identified and quantified (based on FDR $\leq$ 1%) by iTRAQ analysis. Protein with an absolute fold change of > 1.5 or < 0.67, along with a p-value < 0.05 were referred as DEPs. As shown in Table 1, a total of 222 DEPs were detected in the Sham, when compared with the V mice. Among which, 86 were up-regulated, while 136 were down-regulated (Fig. 1**C**). In addition, a total of 149 DEPs were identified in the V mice, relative to the B mice. Among them, 138 were up-regulated and 11 had down-regulated (Fig. 1 **D**).

We also visualized all protein profiles in venn diagram analysis. As shown in Fig. 1**(A, B)**, a total of 77 DEGs were filtered for further analysis (V vs. S and B vs. V, |log2(fold change)| > 1.5, p < 0.05 and unique peptides $\geq$ 2 in one of each group). It showed that Bexarotene induced down-regulation of 1 DEPs and up-regulation of 76 DEPs**.**

3.2. Gene ontology and pathway analyses of DEPs

To better elucidate the molecular and functional attributes of the selected DEPs, we conducted GO enrichment and KEGG pathway analysis in S versus V group and V group versus B group, shown in Fig. 2A-B. Once t-MCAO-induced CIR injury was established, biological process (BP) analysis revealed that a large portion of DEPs were strongly associated with platelet degranulation (P = 8.47 × 10^{-9}), multicellular organismal processes (P = 8.57 × 10^{-9}), and platelet activation (P = 2.97 × 10^{-8}) (Fig. 2a). The assessment of the cell component (CC) found that most DEPs were originated from the myelin sheath (P = 1.89 × 10^{-14}), membrane-bounded vesicles (P = 4.98 × 10^{-11}), and vesicles (P = 8.41 × 10^{-11}) (Fig. 2a). The molecular function (MF) of DEPs were primarily associated with endopeptidase inhibitor activity (P = 4.81 × 10^{-5}), peptidase inhibitor activity (P = 4.80 × 10^{-5}), and in lipid binding (P = 6.31 × 10^{-4}) (Fig. 2A). In B mice, however, the BP analysis showed that most DEPs are involved in synaptic transmission (P = 7.39 × 10^{-8}), glucose metabolic processes (P = 3.49 × 10^{-7}), and cell secretion (P = 4.79 × 10^{-7}) (Fig. 2B). CC analysis of B mice showed prominent origins that include the myelin sheath (P = 9.59 × 10^{-21}), membrane-bounded vesicles (P = 6.75 × 10^{-12}), vesicles (P = 2.28 × 10^{-11}), and so on (Fig. 2B). Lastly, the MF of B mice DEPs played roles in wide pore channel activity (P = 6.97 × 10^{-4}), porin activity (P = 6.97 × 10^{-4}), and purine transmembrane transporter activity (P = 1.13 × 10^{-3}) (Fig. 2B). The KEGG pathway analysis of DEPs in S mice versus V mice revealed correlations with the Huntington's disease (P = 7.61 × 10^{-6}), Parkinson's disease (P = 2.39 × 10^{-5}), complement and coagulation cascades (P = 4.34 × 10^{-5}) (Fig. 2C). B-CIR-injury, on the other hand, was related to microbial metabolism in diverse environments (P = 1.66 × 10^{-7}), calcium signaling (P = 2.24 × 10^{-5}), and proximal tubule bicarbonate reclamation (P = 4.58 × 10^{-5}) (Fig. 2D).

3.3. DEPs in MAPK signaling pathway

To further identify hub proteins associated with the Bexarotene mediated modulation of the MAPK network, we examined the DEPs between B versus V mice. As shown in Table 2, the following MAPK signaling proteins were significantly up-regulated in the B mice versus V mice: heat shock protein 70KD (HSP70), Rabphilin, Calcineurin subunit B type 1, Protein kinase C (PKC) and Protein kinase C beta type (PKCβ). In contrast, C-Jun-amino-terminal kinase-interacting protein 3(JIP3), one of MAPK signaling proteins, was significantly down-regulated in the B mice versus V mice. The peptide spectra and relative ion intensity of JIP3 was illustrated in Fig. 3.

4. Confirmation of the estimated targets

4.1. Low-dose Bexarotene exposure was nontoxic and was protective against OGD injury in HT22 cells

We conducted MTT assay to examine cell toxicity in response to differing concentrations of Bexarotene. In normoxic conditions, cell viability was not affected by low dosage Bexarotene (0.1–9 μM)(P > 0.05, Fig. 1). However, with concentration of 27 μM, cell viability was markedly reduced (P < 0.05, Fig. 4A), suggesting that the toxicity is only associated with high, instead of low, dosage of Bexarotene. Under OGD conditions, 3 and 9 μM Bexarotene markedly enhanced cell viability (P < 0.05, Fig. 4B), with the largest improvement occurring at 9 μM Bexarotene. Hence, 9 μM Bexarotene was chosen for subsequent in vitro experiment ations.

4.2. Effect of OGD/R on the expression of JIP3 and JIP1

To determine whether OGD/R affects the expression of JIP3 and JIP1 genes in HT22 cells, qRT-PCR was conducted to test the expression of these genes at different time points. We demonstrated that from the initiation of re-oxygenation to 12 h after re-oxygenation, JIP3 levels were remarkably increased, as compared to controls (Fig. 5 Ai, P < 0.05). However, JIP1 levels did not alter throughout the examination period, which ranged from the re-oxygenation time till 36 h after reoxygenation (Fig. 5Aii)

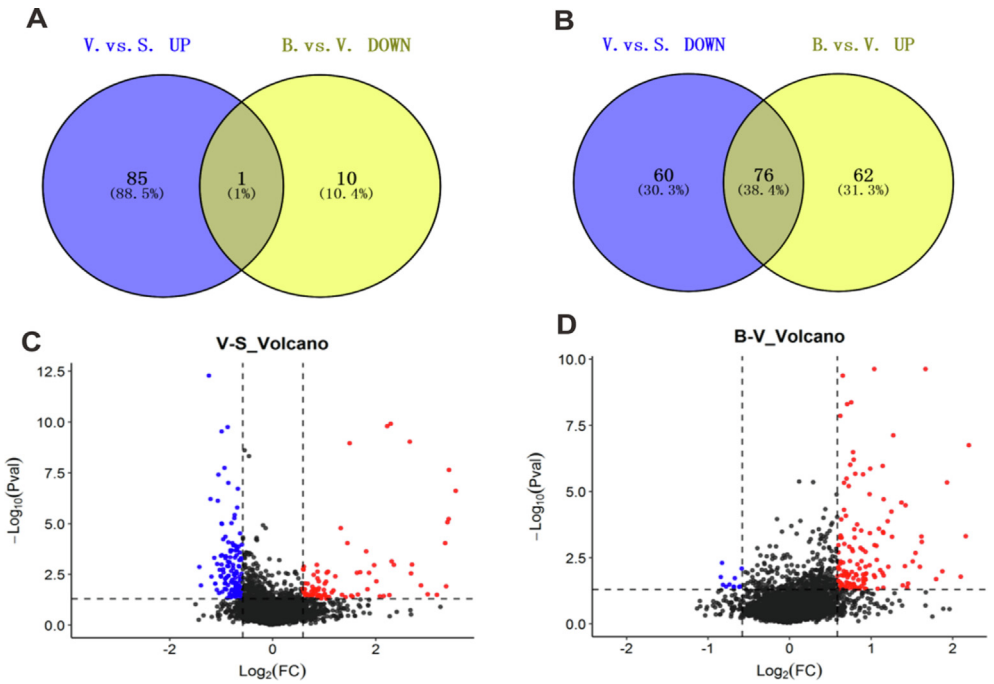

Fig. 1. Bexarotene reversed DEPs induced CIR. (A) The intersection proteins of down-DEPs (V vs. S and B vs. V, up- and down -regulated, respectively). (B)The intersection proteins of up-DEPs (V vs. S and B vs. V, down - and up –regulated, respectively); C-D: Volcano plots of V vs. S and B vs. V. Red nodes refer up-regulation, blue nodes refer down-regulation. DEPs criteria: |log2(fold change)|> 1.5, $p < 0.05$, and unique peptides ≥ 2 (S: Sham-operated , V: vehicle-treated , B: Bexarotene-treated.)

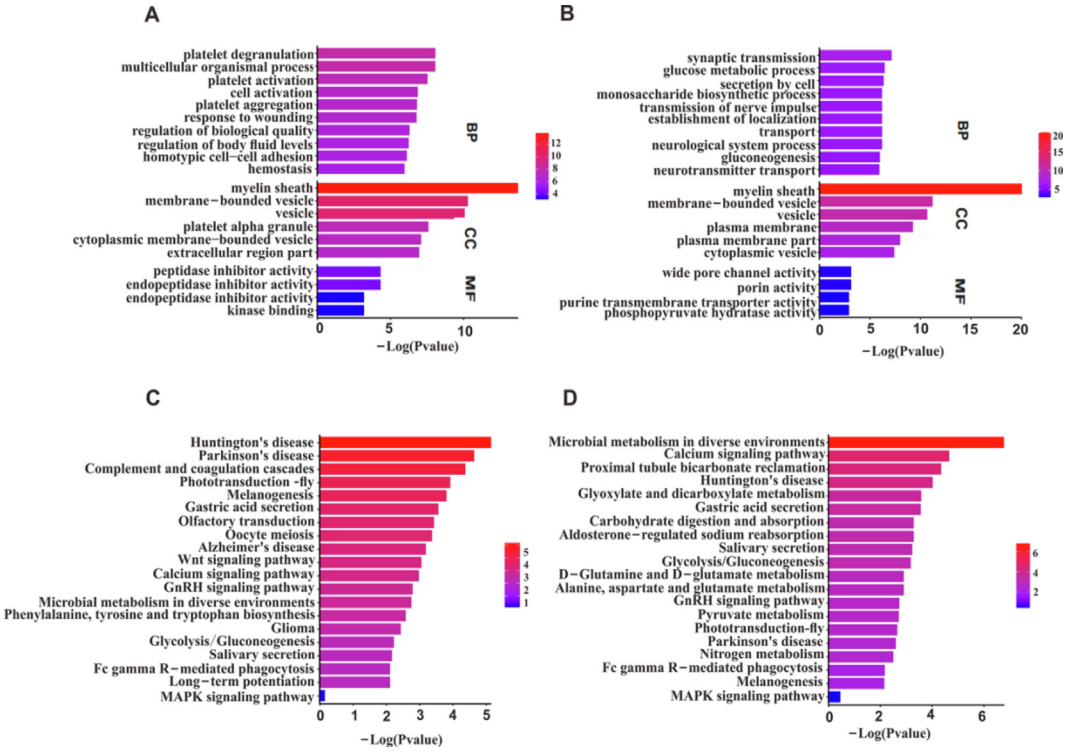

Fig. 2. Results from the DEPs bioinformatics analysis comparing S group versus V group and V group versus B group. **A.** DEPs GO analysis in S group versus V group **B.** DEPs GO analysis in V group versus B group. **C.** DEPs KEGG enrichment in S group versus V- group; **D.** DEPs KEGG enrichment in V group versus B group.

To further verify the influence of OGD/R on JIP3 levels in HT22 cells, both transcript and protein levels were assessed 12 h after OGD/R. We observed remarkable increases in JIP3 gene and protein expressions, relative to controls (Fig. 5B-C, $P < 0.05$). Simultaneously, JIP1 showed no change in gene and protein expression, compared to controls. Given these evidence, OGD/R 12 h was chosen as the intervention time point for subsequent experiments.

4.3. Bexarotene-mediated regulation of HT22 cell activity and LDH leakage rate after OGD/R

The HT22 cell apoptotic rate was investigated via flow cytometry. Relative to controls, OGD/R markedly elevated the HT22 cell apoptotic rate, while Bexarotene treatment significantly decreased cell apoptosis (Fig. 6A, $P < 0.05$).

Table 2
A summary of the differentially expressed MAPK signaling-related proteins in the B-CIR-injury versus V-CIR-injury mice.

NO.	Protein name	Gene name	Uniprot ID	log2 (Fold Change)	p-Value
Up-regulated in MAPK signaling pathway					
1	Heat shock protein 70KD	Hspa 8	Q3UBA6	1.86	2.26792E^{-06}
2	Rabphilin	Rph3a	Q768S5	2.06	0.001058311
3	Calcineurin subunit B type 1	Ppp3r1	Q63810	2.16	0.009214387
4	Protein kinase C	Prkcg	Q3UN66	1.53	0.0263383
5	Protein kinase C beta type	Prkcb	P68404	1.64	0.02910319
Down-regulated in MAPK signaling pathway					
1	C-Jun-amino-terminal kinase-interacting protein 3	Mapk8ip3	Q6P1F1	0.62	0.0041268609

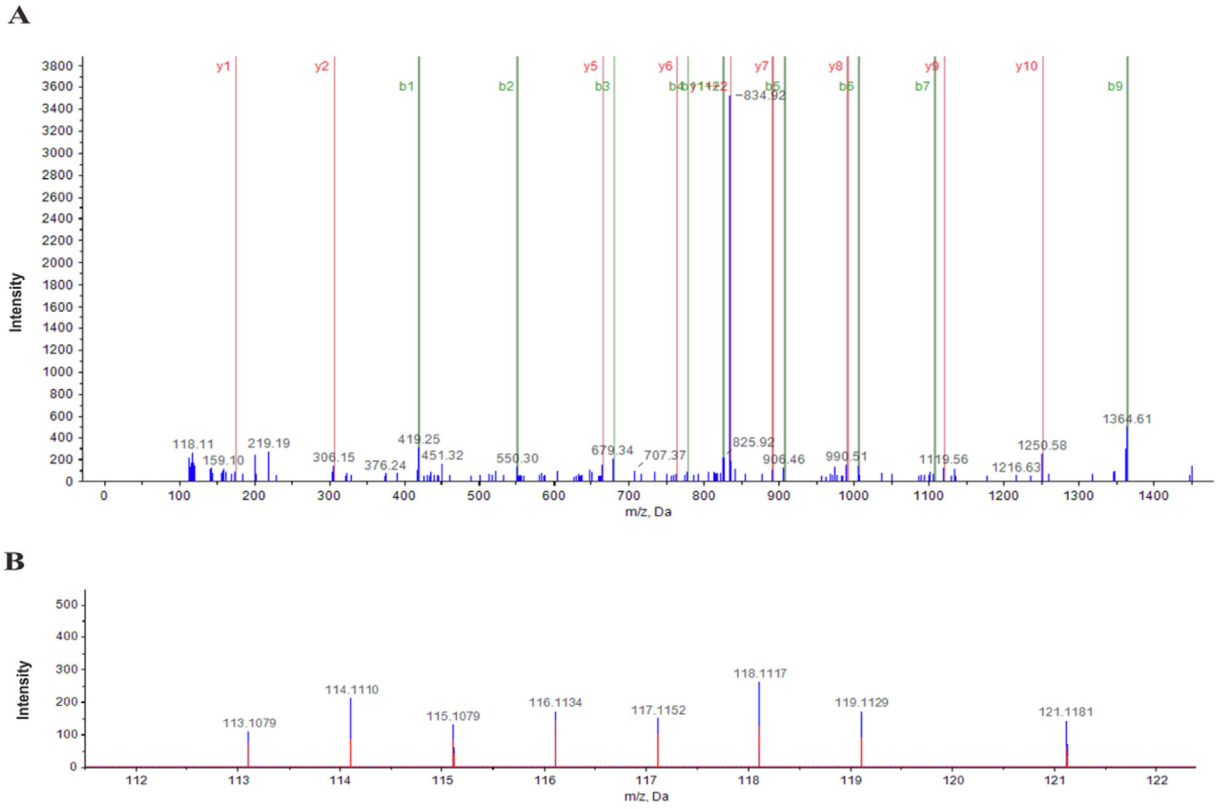

Fig. 3. A-B: Representative differentially expressed proteins (JIP3) peptide spectra and relative ion intensity (A. JIP3 peptide spectra, B. JIP3 relative ion intensity).

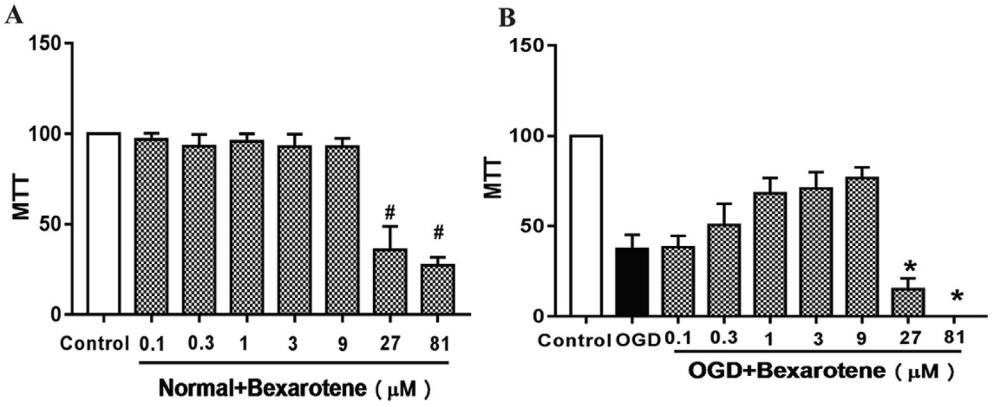

Fig. 4. A-B: Cell viability associated with differing concentrations of Bexarotene on HT22 cells. Data are expressed as mean ± SD, n = 3. $^{\#}P < 0.05$ vs Controls cells, $^{*}P < 0.05$ vs OGD cells.

The HT22 cell survival and cell apoptotic rates were assessed with the MTT and LDH assays, respectively (Fig. 6B-C, P < 0.05). OGD/R stress induced relative low cell survival rate when compared to control (P < 0.05), meanwhile, the LDH leakage rate was drastically high (P < 0.05). However, relative to cells under OGD/R stress, the Bexarotene-treated HT22 cells had markedly

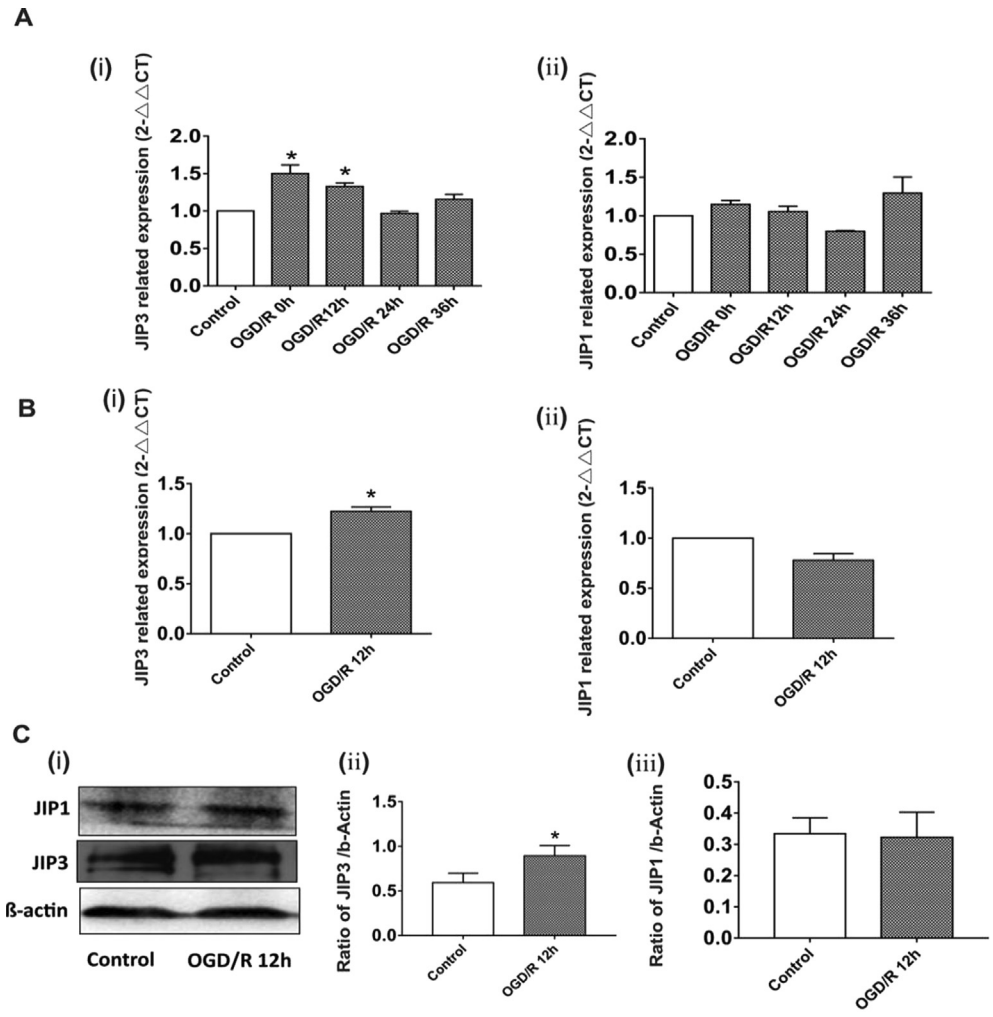

Fig. 5. The expression of JIP3 has significant increased after OGD/R12h. **A:** The qRT-PCR assay was used to measure the JIP3 and JIP1expressionin HT22 cells at different time points after OGD/R. **B**: The qRT-PCR assay was used to measure the JIP3 and JIP1 expression in HT22 cells at 12 h post OGD/R. **C**: The Western blot was used to measure the JIP3 and JIP1 protein levels in HT22 cells at 12 h post OGD/R. Data expressed as mean ± SD, n = 3. *$P < 0.05$ vs. Controls.

enhanced cell survival rates ($P < 0.05$) and significantly reduced LDH leakage rate ($P < 0.05$).

4.4. Bexarotene-mediated regulation of proteins in the JIP3/ JNK/ Caspase 3 signaling pathway

We next examined the Bexarotene-mediated regulation of the OGD/R-related alterations in the JIP3/JNK/Caspase 3 signaling pathway in HT22 cells via western blot. We demonstrated that, relative to controls, the levels of JIP3, p-ASK1, p-JNK, and Cleaved Caspase 3 proteins were remarkably high after OGD/R stress ($P < 0.05$). Moreover, relative to OGD/R stress alone, the Bexarotene-treated cells, under OGD/R stress, exhibited considerably low levels of JIP3, p-ASK1,p-JNK, and Cleaved Caspase 3 proteins (Fig. 7, $P < 0.05$).

4.5. Bexarotene suppresses the JNK/Caspase 3 signaling pathway via reduction in JIP3 expression.

A JIP3 over-expression plasmid was synthesized and then transfected into HT22 cells. To assess the efficiency of the JIP3 over-expression plasmid, we evaluated both transcript and protein levels of JIP3 after transfection. As depicted in Fig 8A-B, JIP3-incorporated HT22 cells exhibited markedly elevated JIP3 mRNA and protein expression, relative to the non-specific control (NC)-JIP3-incorporated cells ($p < 0.05$) Fig. 8C.

In addition, relative to controls, the JIP3, p-ASK1, p-JNK, and Cleaved Caspase 3 protein levels were remarkably increased in OGD/R cells ($P < 0.05$). Moreover, the levels of these proteins were considerably higher in the OGD/R + overexpression (OE)-JIP3 cells, relative to the OGD/R cells ($P < 0.05$). In contrast, in the OGD/R + OE-JIP3 + bexarotene-treated cells, the same protein showed substantial decrease in expression, relative to the OGD/R + OE-JIP3 cells ($P < 0.05$). Given mentioned evidence, Bexarotene attenuates OGD/R injury via inhibition of the JIP3/ASK1/JNK/Caspase3 network in HT22 cells.

5. Discussion

RXR belongs to the NR_2B nuclear receptor family and can form a dimer with peroxisome-activated receptor gamma (PPARγ), a member of the nuclear receptor super family (Giraud-Billoud and Castro-Vazquez 2019, Koshiishi et al., 2019). Being a selective RXR receptor agonist, Bexarotene can stimulate the RXR-PPAR γ dimer formation by activating RXR, and the activated dimer can, in turn, regulate the expression of downstream genes and serve as a variety of haematogenic role (Escudero et al., 2015).

Herein, we analyzed differences in protein expression between the sham, V-CIR-injury, and B-CIR-injury mice, and successfully identified several potential involved proteins. The in-depth bioinformatics analysis revealed 149 DEPs between the B mice and V

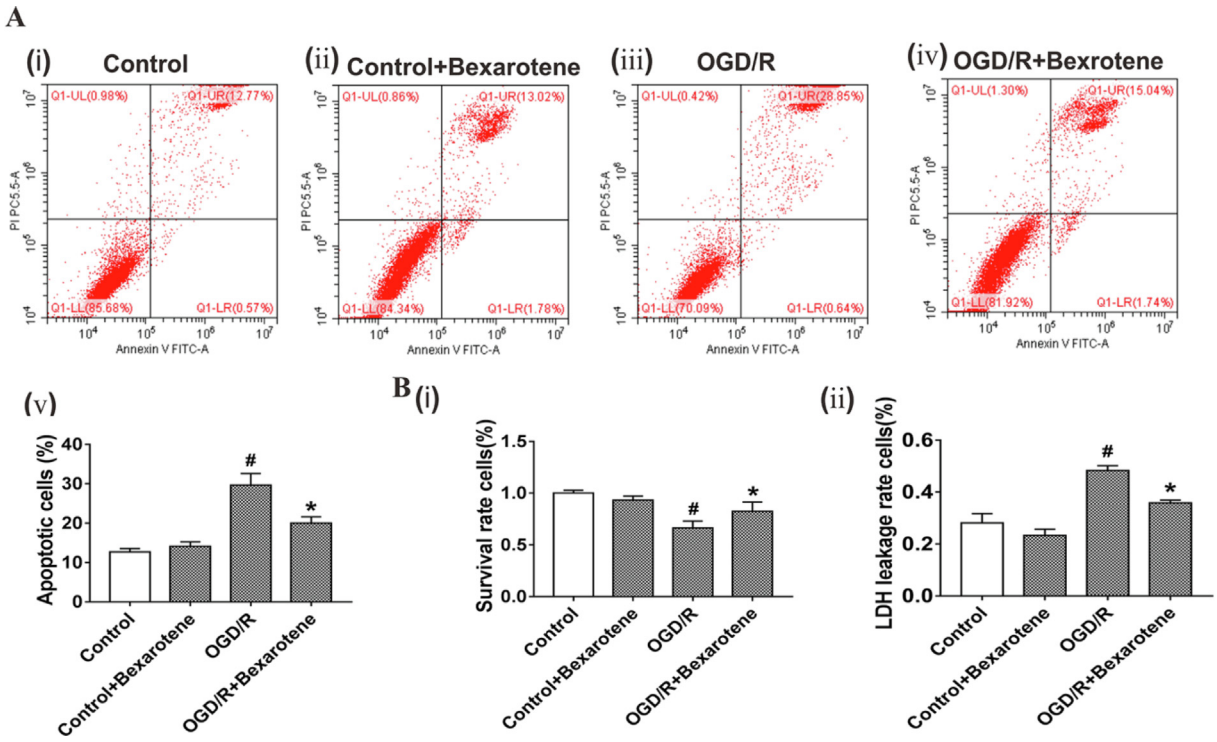

Fig. 6. A: (i)-(iv) Evaluation of HT22 cell apoptotic rate by flow cytometry, (v) Quantification of HT22 cells apoptotic rate. B: (i) HT22 cells survival rate, assessed via MTT, (ii) HT22 cells death rate, evidenced by LDH. Data expressed as mean ± SD. $^{*}P < 0.05$, $^{\#}P < 0.05$vs. Controls.

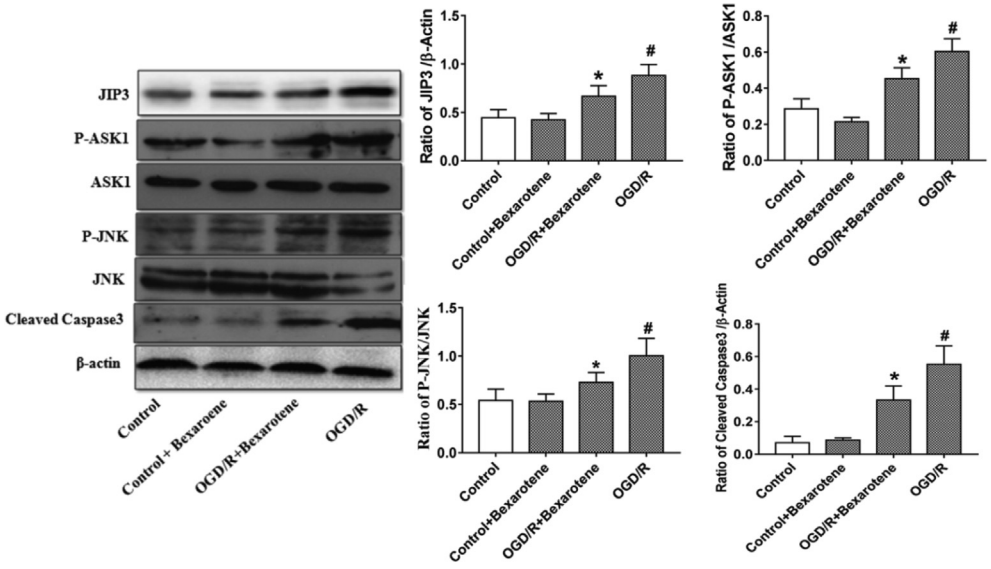

Fig. 7. Alterations in levels of proteins involved in the JIP3/JNK/Caspase 3 signaling pathway in Bexarotene-treated HT22 cells, under OGD/R exposure. Data expressed as mean ± SD. $^{*}P < 0.05$, $^{\#}P < 0.05$vs. Controls.

mice after drug intervention. The GO enrichment analysis showed that DEPs were mainly distributed in the myelin sheath, cytoplasm, cell, and organelle membrane, and participated in biological processes, such as synaptic conduction, enzyme-related energy metabolism, and neurotransmitter transport by regulating enzyme activity and transport of membrane pore proteins. KEGG analysis was performed to further examine the DEPs involved in CIR injury and Bexarotene-mediated protection against CIR injury, and identify their functional role. Our data revealed that the DEPs were mainly distributed in energy metabolism pathways (ex. glycolysis/gluconeogenesis and oxidative stress), calcium signal transduction networks, neurodegenerative axes like Alzheimer's, and mitogen-activat-ed protein kinase (MAPK) signaling pathway.

MAKP signal transduction pathway are extensively involved in various pathophysiological processes, including cell stress, differentiation, apoptosis, inflammation, and so on. These processes often overlap with neuronal pathophysiological alterations after CIR injury. The c-Jun N-terminal kinase (JNK) is an important member of the MAPK family. Our previous study found that Bexarotene against CIR damage via modulation of the JNK/caspase3 activity. However, the underlying mechanism how bexarotene interacts with JNK signaling pathway is still unclear. Proteomic analysis in

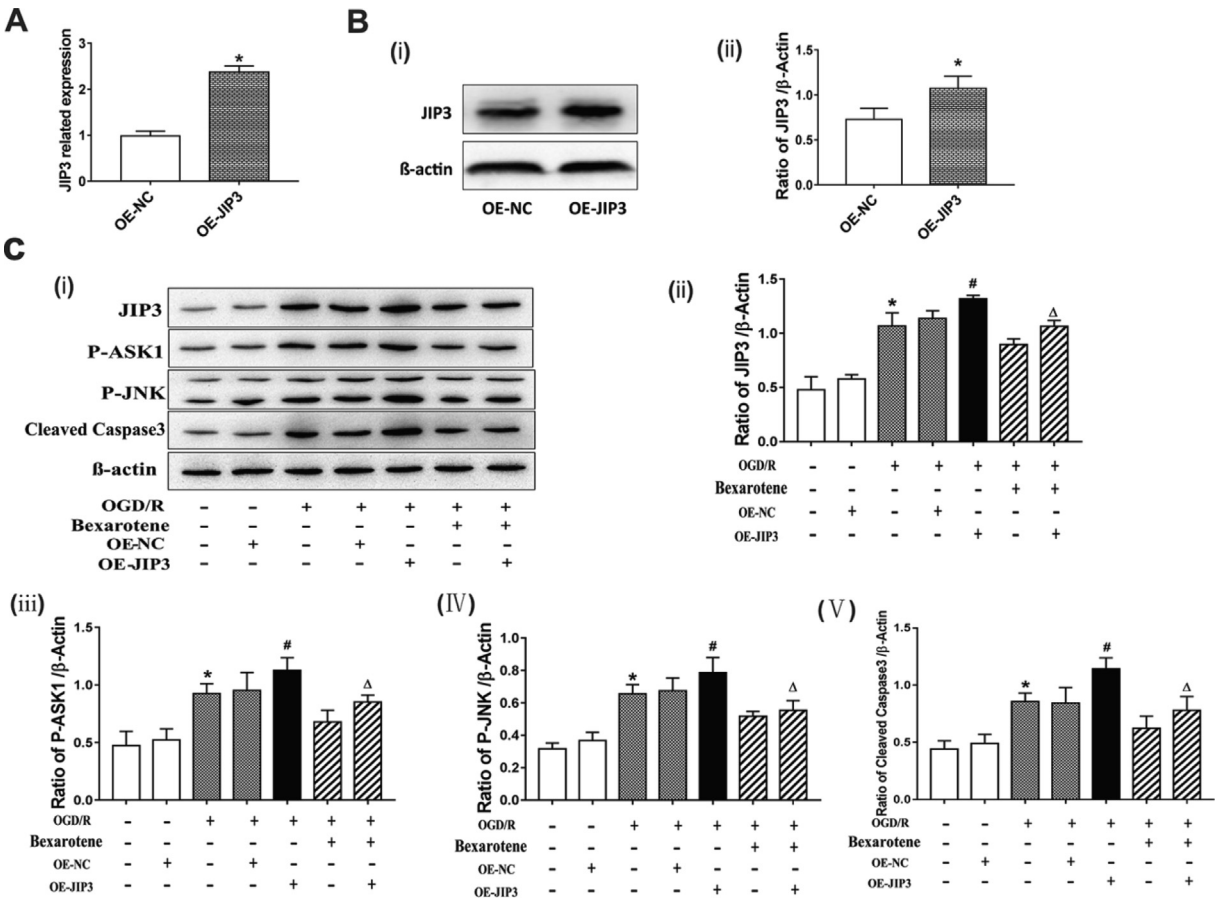

Fig. 8. A-B: Evaluation of the JIP3 transcript and protein expression inHT22 cells transfected with JIP3 overexpression plasmid, relative to NC-JIP3-transfected cells. **C:** Evaluation of proteins involved in the JIP3/ASK1/JNK/Caspase 3 network in JIP3-overexpressing HT22 cells treated with Bexatatene. Data expressed as mean ± SD. $^{*}P < 0.05$ vs. controls, $^{\#}P < 0.05$ vs. OE-NC cells, $^{\triangle}P < 0.05$ vs. OGD/R + OE-JIP3 cells.

this study revealed that Bexarotene treatment can significantly reduce the expression of a key JNK-activated scaffolding protein JIP3, while it has no effect on another scaffolding protein JIP1.

Scaffolding proteins JIP3 and JIP1 serve as a platform for the assembly of molecules in the MAPK network, and they also regulate downstream JNK activity via modulation of the interaction of different molecules (Fu and Holzbaur 2014). JIP3 and JIP1 have vastly different structures and biological functions. In CIR injury, JIP1 interacts with JNK and silk crack the original activated protein kinase kinase (Mitogen – activated protein kinase kinase 7, MKK7) 7 to suppress JNK signaling (Kelkar et al., 2005). This was further confirmed by Xu et al. (Xu et al., 2010) who examined CIR injury in JIP1-overexpressing H9C2 cells. Their results revealed that JIP1 overexpression can significantly inhibit JNK activity (possibly via suppression of JNK nuclear translocation) and dramatically reduce cellular apoptosis. In contrast, JIP1 silencing resulted in a significant increase in JNK expression and cellular apoptosis. Similar response was also observed in pancreatic β cells (Haefliger et al., 2003). Vaishnav et al. reported that Caspase3 disassembles JIP1 at the execution stage of apoptosis, thereby inactivating the JNK signaling pathway (Vaishnav et al., 2011). Given the evidence, it was safe to conclude that JIP1 exerts anti-apoptotic properties via antagonizing JNK signaling pathway.

The top down-regulated protein in MAPK signaling pathway was JIP3, which is an important member of the JNK scaffold protein family JIPs. JIP3 can interact directly with ASK1 and Raf kinases that can phosphorylate and up-regulate MAPK/JNK activity after CIR injury and induce neuronal apoptosis (Song and Lee 2005). Additionally, Matsuura et al. (Matsuura et al., 2002) reported that JIP3 overexpression can activate JNK via ASK1-specific stimulation in PC12 cells. Similarly, Xu et al, (Xu et al., 2010) also revealed JIP3 overexpression can significantly up-regulate JNK activity and promote cell apoptosis, while JIP3 interference can significantly down-regulate JNK activity and ameliorate cell apoptosis. Likewise, Yin et al, (Yin et al., 2016) also showed, in a model of subarachnoid hemorrhage, that JIP3 silencing can vastly improve neurological function of mice while reducing neuronal apoptosis. Based on the above studies, we hypotheses that suppressing the JIP3-induced JNK activation may be an important method to protect against CIR injury. Interestingly, despite large differences in structure and function between JIP3 and JIP1, there is signal crosstalk between them. Song et al. (Song and Lee 2005) reported, in a glucose deprivation model, involving prostate cancer cells, that glucose deprivation rapidly increase interaction between ASK1 and JIP3, promote ASK1 phosphorylation, and activate MKK4. Activated MKK4 then separates from JIP3 and promotes the phosphorylation of JNK, which subsequently inhibits AKT1 and JIP1 activities. Our analysis proved that JIP3 expression was markedly elevated shortly after OGD, which is consistent with published literature. The JIP1 expression, however, did not alter significantly within 36 h of OGD, but it increased after 36 h. This may be due to a time delay related to the signal crosstalk between JIP3 and JIP1. Hence, longer time points are needed to establish JIP1-mediated effects on cells.

To delineate the role of JIP3 in the Bexarotene-mediated protection against OGD/R stress, we over-expressed the JIP3 in HT22 cells. We demonstrated that relative to the cells under OGD/R stress, JIP3-overexpressing cells exhibited markedly elevated levels of JIP3, P-ASK1, P-JNK, and Cleaved Caspase 3. After Bexarotene intervention,

however, the levels of these proteins dropped dramatically. These data suggest that JIP3 can strongly regulate activation of the JNK pathway, which is in accordance with reported literature.

ASK1 is an essential member of the MAPK family and involves in regulation of the apoptotic pathway. In this study, we explored the expression of the scaffolding protein JIP3 and the JIP3-binding protein ASK1 upstream of the JNK pathway. ASK1 activity is usually activated via stress or inflammatory factors and often leads to the activation of the downstream JNK axis (Kawarazaki et al., 2014). Hwang et al, (Hwang et al., 2014) reported that inhibiting ASK1 activity can down-regulate ASK1-MAPK activity, thereby reducing OGD/R-induced cell apoptosis. Given the evidence, it is clear that JIP3 expression increases when cells are injured by OGD/R. Matsuura et al, (Matsuura et al., 2002) reported that the elevated JIP3 can quickly interact with ASK1, causing conformation changes to JIP3, thus promoting the formation of JIP3, ASK1, SEK1/MKK7, and JNK complexes. At this point, JIP3 not only acts like a scaffolding protein, but also dynamically participates in signal transduction in the ASK1-JNK module to accelerate the activation of the JNK-activated apoptotic pathway. Based on our analysis, JIP3 levels and ASK1 phosphorylation were remarkably elevated in OGD/R cells, relative to controls. We also demonstrated simultaneous rises in phosphorylated JNK and Cleaved Caspase 3, which is in accordance with the published reports discussed above. Interestingly, with Bexarotene treatment, JIP3 expression, along with P-ASK1 levels, descended drastically in cells OGD/R stress, relative to controls. Moreover, the Bexarotene-mediated regulation of JIP3 levels was consistent with our proteomics data.

In summary, Bexarotene can down-regulate JIP3 expression under OGD/R stress, inhibit ASK1 and JNK phosphorylation, and reduce the expression level of Cleaved Caspase 3. However, this study is only based on in vitro experiments. It is still unclear whether Bexarotene has the same effects on JIP3 in neuronal insult-related animal models, and further studies will be included in our future work.

Declaration of Competing Interest

The authors declare that they have no known competing financial interests or personal relationships that could have appeared to influence the work reported in this paper.

Acknowledgements

This study was supported by research grants from the Chongqing Science Technology Commission of China (NO: cstc2019jscx-msxmX0096).

References

Katan, M., Luft, A., 2018. Global Burden of Stroke. Semin. Neurol. 38 (02), 208–211.
Baek, S.-H., Noh, A.R., Kim, K.-A., Akram, M., Shin, Y.-J., Kim, E.-S., Yu, S.W., Majid, A., Bae, O.-N., 2014. Modulation of mitochondrial function and autophagy mediates carnosine neuroprotection against ischemic brain damage. Stroke. 45 (8), 2438–2443. https://doi.org/10.1161/STROKEAHA.114.005183.
Campbell, B.C.V., De Silva, D.A., Macleod, M.R., Coutts, S.B., Schwamm, L.H., Davis, S. M., Donnan, G.A., 2019. Ischaemic stroke. Ischaemic stroke. Nat Rev Dis Primers. 5 (1). https://doi.org/10.1038/s41572-019-0118-8.
Escudero, P., Martinez de Maranon, A., Collado, A., et al., 2015. Combined sub-optimal doses of rosuvastatin and bexarotene impair angiotensin II-induced arterial mononuclear cell adhesion through inhibition of Nox5 signaling pathways and increased RXR/PPARalpha and RXR/PPARgamma interactions. Antioxid Redox Signal. 22, 901–920. https://doi.org/10.1089/ars.2014.5969.
Fu, M.-M., Holzbaur, E.L.F., 2014. Integrated regulation of motor-driven organelle transport by scaffolding proteins. Trends Cell Biol. 24 (10), 564–574. https://doi.org/10.1016/j.tcb.2014.05.002.
Giraud-Billoud, M., Castro-Vazquez, A., 2019. Aging and retinoid X receptor agonists on masculinization of female Pomacea canaliculata, with a critical appraisal of imposex evaluation in the Ampullariidae. Ecotoxicol. Environ. Saf. 169, 573–582. https://doi.org/10.1016/j.ecoenv.2018.10.096.
Haefliger, J.A., Tawadros, T., Meylan, L., et al., 2003. The scaffold protein IB1/JIP-1 is a critical mediator of cytokine-induced apoptosis in pancreatic beta cells. J. Cell Sci. 116, 1463–1469. https://doi.org/10.1242/jcs.00356.
Huuskonen, M.T., Loppi, S., Dhungana, H., Keksa-Goldsteine, V., Lemarchant, S., Korhonen, P., Wojciechowski, S., Pollari, E., Valonen, P., Koponen, J., Takashima, A., Landreth, G., Goldsteins, G., Malm, T., Koistinaho, J., Kanninen, K.M., 2016. Bexarotene targets autophagy and is protective against thromboembolic stroke in aged mice with tauopathy. Sci. Rep. 6 (1). https://doi.org/10.1038/srep33176.
Hwang, S.G., Shim, J., Choi, E.-J., 2014. CIIA negatively regulates neuronal cell death induced by oxygen-glucose deprivation and reoxygenation. Mol. Cell Biochem. 397 (1-2), 139–146. https://doi.org/10.1007/s11010-014-2181-5.
Kawarazaki, Y., Ichijo, H., Naguro, I., 2014. Apoptosis signal-regulating kinase 1 as a therapeutic target. Expert Opin. Ther. Targets. 18 (6), 651–664. https://doi.org/10.1517/14728222.2014.896903.
Kelkar, N., Standen, C.L., Davis, R.J., 2005. Role of the JIP4 scaffold protein in the regulation of mitogen-activated protein kinase signaling pathways. Mol. Cell Biol. 25 (7), 2733–2743. https://doi.org/10.1128/MCB.25.7.2733-2743.2005.
Koshiishi, C., Kanazawa, T., Vangrevelinghe, E., Honda, T., Hatakeyama, S., 2019. Identification and characterization of a phenyl-thiazolyl-benzoic acid derivative as a novel RAR/RXR agonist. Heliyon. 5 (11), e02849. https://doi.org/10.1016/j.heliyon.2019.e02849.
Liu, H., Liu, S., Tian, X., Wang, Q., Rao, J., Wang, Y., Xiang, F., Zheng, H., Xu, L.u., Dong, Z., 2019. Bexarotene Attenuates Focal Cerebral Ischemia-Reperfusion Injury via the Suppression of JNK/Caspase-3 Signaling Pathway. Neurochem. Res. 44 (12), 2809–2820. https://doi.org/10.1007/s11064-019-02902-5.
Matsuura, H., Nishitoh, H., Takeda, K., Matsuzawa, A., Amagasa, T., Ito, M., Yoshioka, K., Ichijo, H., 2002. Phosphorylation-dependent scaffolding role of JSAP1/JIP3 in the ASK1-JNK signaling pathway. A new mode of regulation of the MAP kinase cascade. J. Biol. Chem. 277 (43), 40703–40709. https://doi.org/10.1074/jbc.M202004200.
Song, J.J., Lee, Y.J., 2005. Cross-talk between JIP3 and JIP1 during glucose deprivation: SEK1-JNK2 and Akt1 act as mediators. J. Biol. Chem. 280 (29), 26845–26855. https://doi.org/10.1074/jbc.M502318200.
Vaishnav, M., MacFarlane, M., Dickens, M., 2011. Disassembly of the JIP1/JNK molecular scaffold by caspase-3-mediated cleavage of JIP1 during apoptosis. Exp. Cell Res. 317 (7), 1028–1039. https://doi.org/10.1016/j.yexcr.2011.01.011.
Xu, B., Zhou, Y., O, K., Choy, P.C., Pierce, G.N., Siow, Y.L., 2010. Regulation of stress-associated scaffold proteins JIP1 and JIP3 on the c-Jun NH2-terminal kinase in ischemia-reperfusion. Can. J. Physiol. Pharmacol. 88 (11), 1084–1092.
Xu, L.u., Cao, F., Xu, F., He, B., Dong, Z., Koval, M., 2015. Bexarotene reduces blood-brain barrier permeability in cerebral ischemia-reperfusion injured rats. PLoS One. 10 (4), e0122744. https://doi.org/10.1371/journal.pone.0122744.
Yin, C., Huang, G.-f., Sun, X.-C., Guo, Z., Zhang, J.H., 2016. Tozasertib attenuates neuronal apoptosis via DLK/JIP3/MA2K7/JNK pathway in early brain injury after SAH in rats. Neuropharmacology. 108, 316–323. https://doi.org/10.1016/j.neuropharm.2016.04.013.
Zhong, J., Jiang, L.i., Huang, Z., Zhang, H., Cheng, C., Liu, H., He, J., Wu, J., Darwazeh, R., Wu, Y., Sun, X., 2017. The long non-coding RNA Neat1 is an important mediator of the therapeutic effect of bexarotene on traumatic brain injury in mice. Brain Behav Immun. 65, 183–194. https://doi.org/10.1016/j.bbi.2017.05.001.
Zhou, F., Gao, S., Wang, L., Sun, C., Chen, L.u., Yuan, P., Zhao, H., Yi, Y.i., Qin, Y., Dong, Z., Cao, L., Ren, H., Zhu, L., Li, Q., Lu, B., Liang, A., Xu, G.-T., Zhu, H., Gao, Z., Ma, J., Xu, J., Chen, X.u., 2015. Human adipose-derived stem cells partially rescue the stroke syndromes by promoting spatial learning and memory in mouse middle cerebral artery occlusion model. Stem Cell Res Ther. 6 (1). https://doi.org/10.1186/s13287-015-0078-1.